

Enhancement in Photoluminescence on Mg Substitution in $\text{Mg}_x\text{Sr}_{1-x}\text{Al}_2\text{O}_4$: Eu, Nd

H. Ryu¹ and K.S. Bartwal^{*1,2}

¹Energy Materials Research Centre, Korea Research Institute of Chemical Technology, P.O. Box 107, Yuseong, Daejeon 305-600, Republic of Korea

²Permanent address: Laser Materials Development & Devices Division, Raja Ramanna Centre for Advanced Technology, Indore-452 013, India

Abstract: Strontium aluminate, SrAl_2O_4 is well-known phosphor host material with spinel structure. Mg substituted compositions, $\text{Mg}_x\text{Sr}_{1-x}\text{Al}_2\text{O}_4$: Eu, Nd (with $x = 0.05 - 0.25$) were prepared by solid-state reaction method. Effect of Mg substitution on structure and photoluminescence was investigated. Prepared compositions were characterized for the phase and crystallinity by powder X-ray diffraction. The micro-structural investigations were carried out by transmission electron microscopy (TEM) technique. Photoluminescence characteristics show the intense emission for $\text{MgSrAl}_2\text{O}_4$:Eu²⁺, Nd³⁺ in the green region ($\lambda_{\text{max}} = 512$ nm) with long persistence. The green emission corresponds to transitions from $4f^6 5d^1$ to $4f^7$ of Eu²⁺ ion.

PACS: 78.55.-m; 78.55.Hx.

INTRODUCTION

A new generation of persistent luminescent phosphors, Eu²⁺ doped alkaline-earth aluminates, MAl_2O_4 : Eu²⁺ (M = Ca, Ba, Sr), have been developed to replace the traditional sulphide phosphors, ZnS: Cu [1-3]. Long persistence materials are needed in applications like signing and display [4, 5]. For these purposes rare-earth ion doping in alkaline-earth aluminates is well established. Aluminates generally generate more defect related traps when they are doped with rare-earth ions. Several aluminate compositions are investigated and used as photoluminescence, catholuminescence and plasma display panel phosphors for their high quantum efficiency in the visible region. The emission of Eu²⁺ is very strongly dependent on the host lattice and can occur from ultraviolet to the red region of the electro-magnetic spectrum [6-8]. Notably barium and strontium aluminates have been reported to be good host materials. In the SrO–Al₂O₃ system, four well-known phosphor hosts, SrAl_2O_4 [9], $\text{SrAl}_{12}\text{O}_{19}$ [10], $\text{Sr}_2\text{Al}_6\text{O}_{11}$ and $\text{Sr}_4\text{Al}_{14}\text{O}_{25}$ [11] exist. Green-emitting SrAl_2O_4 that has been co-doped with Dy³⁺ and Eu²⁺ ions and recrystallized with B₂O₃ flux has been regarded as a useful long persistence phosphor [12-15]. Strontium aluminate, SrAl_2O_4 can be used safely as phosphorescent pigment for luminous watches, clocks and cold-lighting that emits no infrared radiation. Katsumata *et al.* [16] have reported that among the four strontium aluminates mentioned above, only the first two compounds are found to exhibit phosphorescence when co-activated by Eu²⁺ and Dy³⁺, with the emission peak around 520 nm and 400 nm, respectively. The emission studies on BaAl_2O_4 :Eu²⁺, CaAl_2O_4 :Eu²⁺, Nd³⁺ and their solid solutions have been reported earlier [17-21].

We have prepared and investigated SrAl_2O_4 based materials by substituting Sr with Mg and co-doping of Eu²⁺ and Nd³⁺ ions as activator and sensitizer respectively. The single phase limit of Mg in SrAl_2O_4 :Eu²⁺, Nd³⁺ phosphor was investigated using powder X-ray diffraction. High-resolution TEM was used to understand the microstructure of the material. Photoluminescence characteristics were investigated by measuring excitation and emission spectrum of these compositions.

EXPERIMENTAL DETAILS

Solid-state synthesis method was used to prepare the compositions $\text{Mg}_x\text{Sr}_{1-x}\text{Al}_2\text{O}_4$:Eu²⁺, Nd³⁺ ($x = 0.05, 0.10, 0.15, 0.20$ and 0.25). High purity (Aldrich, 99.99%) raw materials; MgO, SrCO₃, Al₂O₃, Eu₂O₃, Nd₂O₃ and B₂O₃ in appropriate quantities were used for preparation of the charge. The composition for each material was weighted in proper stoichiometric ratios. Eu₂O₃ and Nd₂O₃ were mixed with the charge as activator and sensitizer ions respectively. The concentration of active ions Eu²⁺ and Nd³⁺ was optimized separately. It was found that the combination of 1 mol% Eu₂O₃ and 2 mol% Nd₂O₃ is best for the higher photoluminescence in this material. The stoichiometric charge was mixed thoroughly with ethanol in an agate mortar and the resulting slurry was dried at 80 °C in a vacuum oven. The mixed and ground powders were sintered at 1000 °C for 6h in an air atmosphere. The resulting powders were annealed at 1300 °C for 4h in a reducing atmosphere (5% H₂ and 95% N₂) to ensure complete reduction of Eu³⁺ to Eu²⁺. The phase and crystallinity of the synthesized compositions were investigated by powder XRD using Rigaku D/MAX-2200V diffractometer with Cu K_α radiation. High-resolution TEM studies were done to investigate the crystallinity and defect structure of the phosphor. Sample for TEM observation was prepared by suspending the particles in ethanol by ultrasonication and drying a drop of the suspension on a carbon coated cop-

*Address correspondence to this author at the Energy Materials Research Centre, Korea Research Institute of Chemical Technology, P.O. Box 107, Yuseong, Daejeon 305-600, Republic of Korea; Tel: +82-42-860-7376; Fax: +82-42-861-4245; E-mail: bartwalks@yahoo.co.in

per grid. Philips Tecnai G²-20 (FEI) electron microscope operating at 200 kV was used for TEM experiments. The photoluminescence (PL) emission spectra were taken on Perkin-Elmer LS50B luminescence spectrometer. Each sample was loaded into a circular holder and excited with 254 nm radiation from a pulsed xenon lamp. The emission spectra were scanned in the range of wavelengths from 360 to 700 nm. To measure the excitation spectra, the analyzer monochromator was set to the maximum wavelength of the emission spectra and then an excitation monochromator was scanned in the range of 200 to 400 nm. The decay time was recorded using a pulsed Xenon lamp and oscilloscope.

RESULTS AND DISCUSSION

Phosphor compositions in the series $\text{Mg}_x\text{Sr}_{1-x}\text{Al}_2\text{O}_4:\text{Eu}^{2+}, \text{Nd}^{3+}$ (with $x = 0.05, 0.10, 0.15, 0.20$ and 0.25) were prepared. The Eu^{2+} and Nd^{3+} concentrations in $\text{Mg}/\text{SrAl}_2\text{O}_4$ were optimized independently and were kept at 1 mol% and 2 mol% respectively. The Mg/Sr solid-solution range was optimized with the help of powder XRD. The parent host aluminates with general formula MAI_2O_4 ($M = \text{Ca}, \text{Ba}, \text{Sr}$) are formed with a three-dimensional frame-work of corner sharing AlO_4 tetrahedra. Each oxygen ion is shared by two aluminum ions so that each tetrahedron has one net negative charge. The charge balance is achieved by the large divalent cations like $\text{Ba}^{2+}, \text{Sr}^{2+}, \text{Ca}^{2+}$ etc. which occupy interstitial site within the tetrahedral frame-work. The tetrahedra frame-work is isostructural with the tridymite structure. Fig. (1) shows the representative XRD patterns taken for $\text{Mg}_x\text{Sr}_{1-x}\text{Al}_2\text{O}_4:\text{Eu}^{2+}, \text{Nd}^{3+}$ compositions (with $x = 0, 0.10$ and 0.25). The XRD pattern for parent SrAl_2O_4 ($x=0$) was given for comparison. The XRD patterns show the monoclinic phase diffraction peaks of parent SrAl_2O_4 . The lattice parameters for the parent SrAl_2O_4 were calculated from XRD data and are matching well with the JCPDS data file (PDF# 74-0794). The lattice parameters calculated were for monoclinic SrAl_2O_4 , $a = 8.441 \text{ \AA}$, $b = 8.812 \text{ \AA}$ and $c = 5.158 \text{ \AA}$. A little amount of doped rare-earth active ions Eu^{2+} and Nd^{3+} has almost no effect on the basic crystal structure of SrAl_2O_4 . It is revealed from the XRD patterns that there is no extra peak for Mg up to the composition of $x=0.25$. There is no mixed phase present in the prepared material. It suggests that the substitution of Sr^{2+} (1.18 \AA) by Mg^{2+} (0.72 \AA) is smooth though the size difference is large. The prepared mixed compositions retain the parent spinel structure. The Sr^{2+} and Eu^{2+} are very similar in their ionic sizes (1.21 \AA and 1.20 \AA , respectively). This means when occupied by Eu^{2+} ions, the two different Sr^{2+} sites will have a quite similar local distortion, so that the Eu^{2+} ions located at the two sites will have similar environment. The second dopant Nd^{3+} ion (1.16 \AA) also occupies the Sr^{2+} site.

Transmission electron microscopy (TEM) is the best tool to investigate the local structure and defect structure of the material. TEM studies were conducted to investigate the morphology and the crystalline defects in the synthesized material. Fig. (2a-c) shows the representative high-resolution (HRTEM) bright-field micrographs for the samples with $x = 0.05, 0.15$ and 0.25 . The corresponding selected area electron diffraction (SAD) patterns are inserted on the micrographs. There is no indication in the micrograph for the presence of secondary phases. The clarity of the fringe patterns in high-

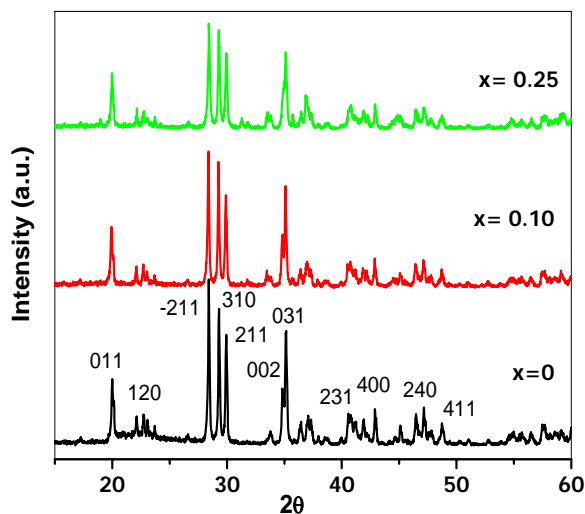


Fig. (1). Representative XRD patterns for $\text{Mg}_x\text{Sr}_{1-x}\text{Al}_2\text{O}_4:\text{Eu}^{2+}, \text{Nd}^{3+}$ ($x = 0, 0.10$ and 0.25).

resolution micrographs shows the synthesized material crystallizes in single phase. Also the clear and strong diffraction spots in the SAD patterns are indicative of the crystalline particles having sufficient sizes. However the streaks along spots and diffuse scattering can be seen in the SAD patterns for higher x values. These streaks along the diffraction spots and faint diffuse scattering are indicative of the point defects produced by excess of Mg concentrations. The faint streaks with diffuse scattering as the elongation of basic spots can be seen for $x = 0.15$ in Fig. (2b), which further increases for $x = 0.25$ in Fig. (2c). These HRTEM results suggest that the mixed compositions retain the parent spinel phase till the composition with $x = 0.25$. This further supports the XRD results where there is no extra peak was found. Only slightly enhanced point defects were observed in higher Mg/Sr substitution concentrations.

Photoluminescence studies were carried out on the prepared phosphor compositions. All the phosphor compositions exhibit green emission when excited by UV light. The appearance of green emission indicates that the matrix retain the parent phosphor host. The activator ion Eu is in divalent Eu^{2+} , green emission state. The excitation and emission spectra for $\text{Mg}_x\text{Sr}_{1-x}\text{Al}_2\text{O}_4:\text{Eu}^{2+}, \text{Nd}^{3+}$ phosphors for different values of x (0.05, 0.10, 0.15, 0.20 and 0.25) are shown in Fig. (3a, b). The excitation spectra of $\text{Mg}_x\text{Sr}_{1-x}\text{Al}_2\text{O}_4:\text{Eu}^{2+}, \text{Nd}^{3+}$ phosphor (Fig. 3a) show two broad bands extending between 220 to 280 nm and 300 to 390 nm corresponds to the crystal field splitting of the Eu^{2+} d-orbital. The emission has a symmetrical band peak at 512 nm for all the compositions (Fig. 3b). These emissions are attributed to the typical $4f^65d^1 - 4f^7$ transition of Eu^{2+} ion [13]. The Nd^{3+} co-doping in these phosphor materials creates the deep trapping levels. The compositions with higher Mg concentrations show higher excitation and emission intensities. It was observed that when the phosphor material with composition of Mg at $x = 0.15$, the emission spectrum has highest intensity (Fig. 3b). This combination of Sr and Mg also shows higher excitation intensity and longer decay time. The Mg concentration above this optimum value shows lowering of the excitation and emission intensities. It is understood that the sensitizer

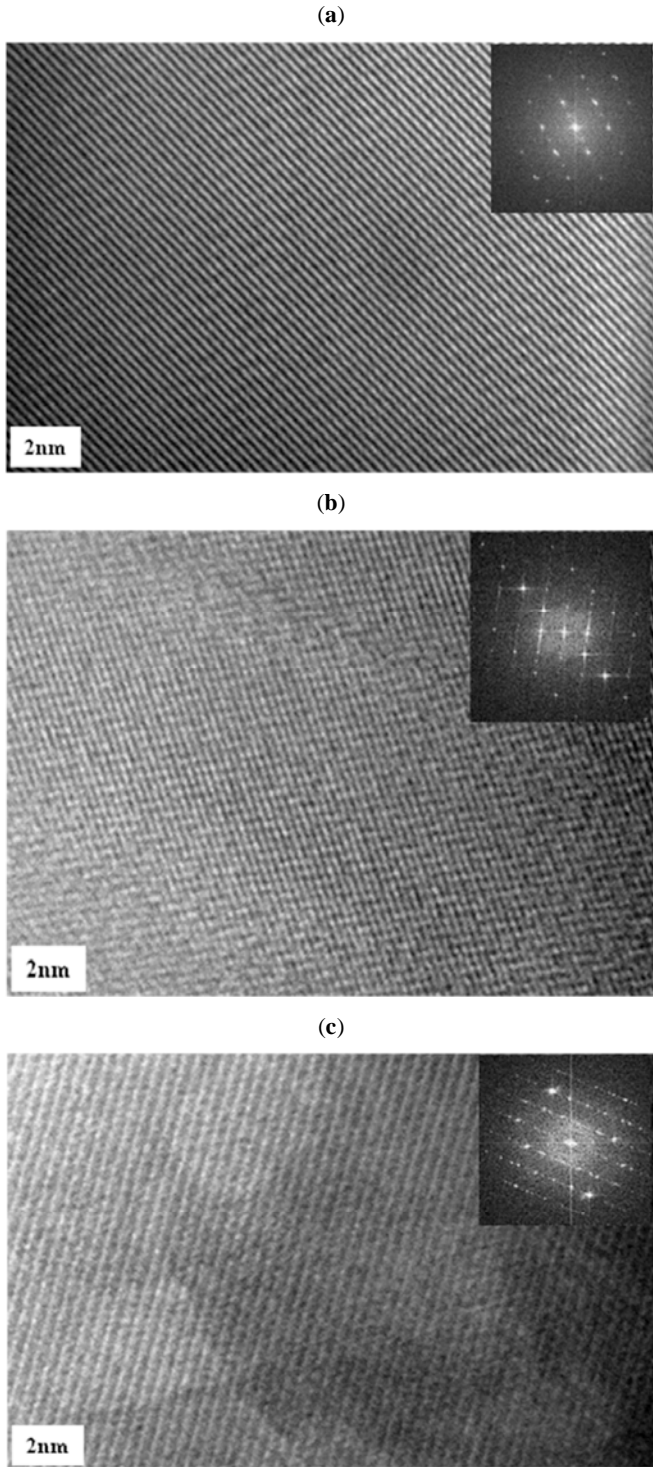


Fig. (2). Representative HRTEM micrographs for $Mg_xSr_{1-x}Al_2O_4:Eu^{2+}, Nd^{3+}$, (a) $x=0.05$, (b) $x=0.15$ and (c) $x=0.25$. Corresponding SAD patterns are inserted in the micrograph.

ion Nd^{3+} act as traps of holes and the trap levels lie near the valence band [18, 22]. Electron-hole pairs are produced in Eu^{2+} ions, when excited by the excitation light source and the Nd^{3+} traps capture some of the free holes moving in the valence band. When the excitation source is cut off, some holes captured by the Nd^{3+} traps are thermally released slowly and relaxed to the excited state of Eu^{2+} , finally, returning to the

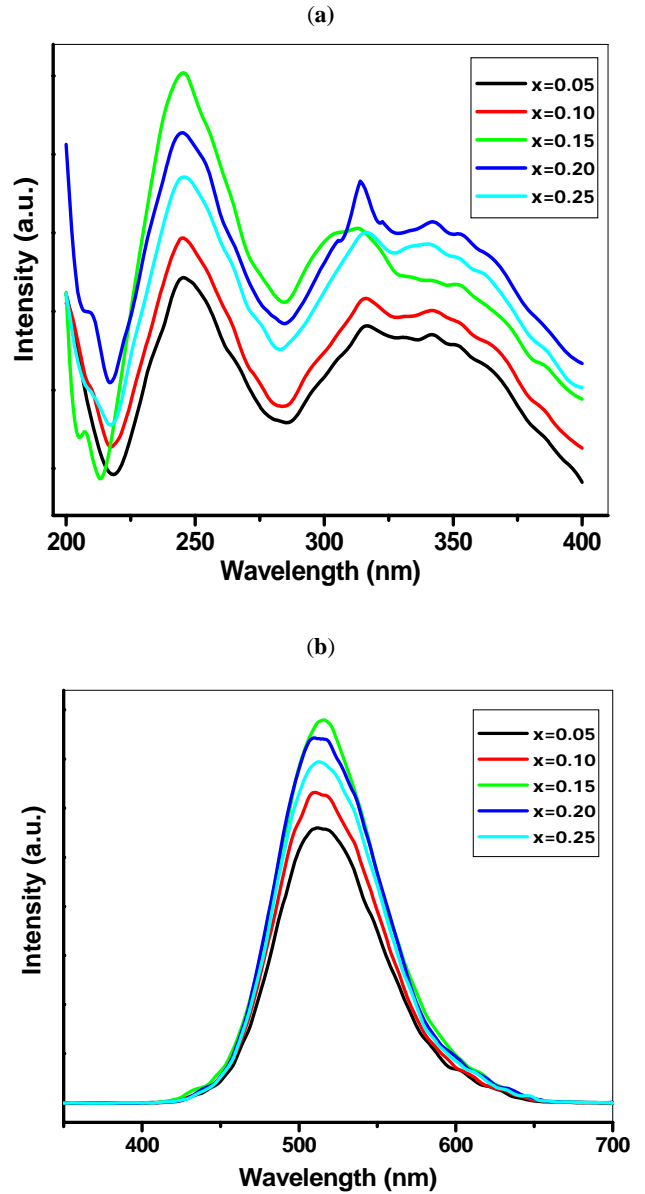


Fig. (3). Excitation (a) and emission (b) spectra for $Mg_xSr_{1-x}Al_2O_4:Eu^{2+}, Nd^{3+}$ ($x=0.05, 0.10, 0.15, 0.20$ and 0.25).

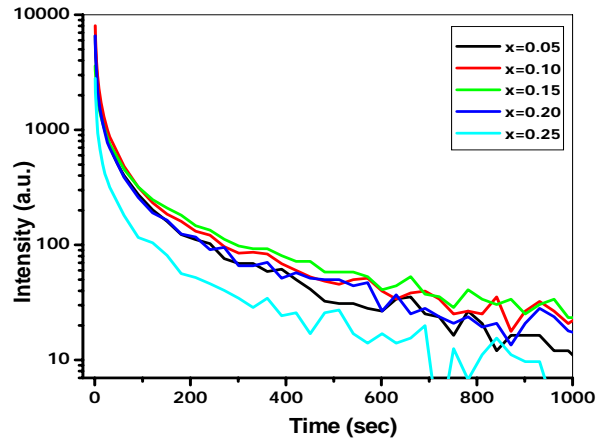


Fig. (4). Decay curves for $Mg_xSr_{1-x}Al_2O_4:Eu^{2+}, Nd^{3+}$ ($x=0.05, 0.10, 0.15, 0.20$ and 0.25).

ground state of Eu^{2+} accompanied with emitting light. The mechanism of the long persistence is due to the holes trapped-transported-detrapped process [13, 14]. This is the reason why doubly doped phosphor materials maintain a long persistent decay time after the excitation is cut off. The prepared phosphor compositions show long decay time when the powders were efficiently activated by a pulsed Xenon lamp for 15 min. When the source lamp was switched off, the intensity of the persistence decreased rapidly and finally formed a stable long persistent emission for several minutes. The persistent luminescence curves for $\text{Mg}_x\text{Sr}_{1-x}\text{Al}_2\text{O}_4:\text{Eu}^{2+}, \text{Nd}^{3+}$ ($x = 0.05, 0.10, 0.15, 0.20$ and 0.25) are shown in Fig. (4). The decay curves are plotted in log scale so that the time dependence is clearer. The curves show that the trend of increasing the decay time with increasing Mg concentration, highest at the optimized composition of $x = 0.25$. When the substitution concentration reaches above this, the decay time starts decreasing. The Nd^{3+} incorporation creates deep traps in the form of hole trapping levels near the valence band. Therefore, when the excitation source is switched off, the relaxation of these secondary ions from deep traps is very slow; this leads to the long persistence of the phosphor. The optimized composition $\text{Mg}_x\text{Sr}_{1-x}\text{Al}_2\text{O}_4:\text{Eu}^{2+}, \text{Nd}^{3+}$ ($x = 0.15$) with Eu (1 mol%) and Nd (2 mol%) sufficiently good photoluminescence with longer persistent time. It has been found from the detailed studies on these visible phosphors [19-22] that the role of second rare-earth is important to enhance the decay time and the combination of the substitution by alkaline earth element dictates the luminescence intensity. This trend can be a guideline to set boundary conditions to look for the desired composition. The perfect combination among these doping and substitution is still being studied in-depth to find out the most state-of-the-art composition.

CONCLUSIONS

Green phosphors $\text{Mg}_x\text{Sr}_{1-x}\text{Al}_2\text{O}_4:\text{Eu}^{2+}, \text{Nd}^{3+}$ ($x = 0.05-0.25$) were synthesized by solid-state reaction method. Powder XRD analysis shows that the synthesized phosphor compositions with varying Mg concentration retain the parent SrAl_2O_4 monoclinic crystal structure. TEM investigations also indicate that the parent spinel structure was retained on Mg substitution. The TEM study shows that the local area disorder (point defects) is introduced due to excess substitution concentration. PL characteristics was investigated for varying Mg concentrations and it was optimized that $\text{Mg}_x\text{Sr}_{1-x}\text{Al}_2\text{O}_4:\text{Eu}^{2+}, \text{Nd}^{3+}$ ($x = 0.15$) has the highest PL intensity and longer persistent time.

ACKNOWLEDGEMENT

One of the authors (K. S. Bartwal) is grateful to the Korean Federation of Science and Technology Societies (KOFST) for financial support under the Brain Pool Program.

REFERENCES

- Murayama Y, Takeuchi N, Aoki Y, Matsuzawa T. Phosphorescent phosphor. US Patent 5424006, June 13, 1995.
- Nakamura T, Kaiya K, Takahashi N, Matsuzawa T, Rowlands CC, Beltran-Lopez V, Smith GM, Riedi PC. High frequency EPR of europium (II)-doped strontium aluminate phosphors. *J Mater Chem* 2000; 10: 2566-9.
- Qiu J, Gaeta AL, Hirao K. Long-lasting phosphorescence in oxygen-deficient Ge-doped silica glasses at room temperature. *Chem Phys Letts* 2001; 333: 236-41.
- Jia D, Wang XJ, vander Kolk E, Yen WM. Site dependent thermoluminescence of long persistent phosphorescence of $\text{BaAl}_2\text{O}_4:\text{Ce}^{3+}$. *Opt Commun* 2002; 204: 247-51.
- Jeong IK, Park HL, Mho SI. Photoluminescence of ZnGa_2O_4 mixed with InGaZnO_4 . *Solid State Commun* 1998; 108: 823-6.
- Kityk IV, Wasylak J, Dorosz D, Kucharski J. Eu^{3+} -doped glass materials for red luminescence. *Opt Laser Tech* 2001; 33: 157-60.
- Kityk IV, Sahraoui B. Photo induced two-photon absorption and second-harmonic generation in $\text{As}_2\text{Te}_3\text{-CaCl}_2\text{-PbCl}_2$ glasses. *Phys Rev B* 1999; 60: 942-9.
- Brik MG. Complex study of the crystal field splitting, "ligand-impurity ion" charge transfer transitions and high lying 4f-6s intraconfigurational transitions for all trivalent lanthanides in $\text{Cs}_2\text{NaYCl}_6$ crystal. *J Alloys Compd* 2008; 454: 38-45.
- Abbruscato V. Optical and Electrical Properties of $\text{SrAl}_2\text{O}_4:\text{Eu}^{2+}$. *J Electrochem Soc* 1971; 118: 930-3.
- Stevens ALN, Schrama-de Pauw ADM. Eu^{2+} Luminescence in Hexagonal Aluminates Containing Large Divalent or Trivalent Cations. *J Electrochem Soc* 1976; 123: 691-7.
- Smets B, Rutten J, Hoeks G, Verlijndonk J. $2\text{SrO} \cdot 3\text{Al}_2\text{O}_3:\text{Eu}^{2+}$ and $1.29(\text{Ba,Ca})\text{O} \cdot 6\text{Al}_2\text{O}_3:\text{Eu}^{2+}$ two new blue -emitting phosphors. *J Electrochem Soc* 1989; 136: 2119-23.
- Nag A, Kuty TRN. The mechanism of long phosphorescence of $\text{SrAl}_{2-x}\text{B}_x\text{O}_4$ ($0 < x < 0.2$) and $\text{Sr}_4\text{Al}_{14-x}\text{B}_x\text{O}_{25}$ ($0.1 < x < 0.4$) co-doped with Eu^{2+} and Dy^{3+} . *Mater Res Bull* 2004; 39: 331-42.
- Clabau F, Rocquefelte X, Jobic S, et al. Mechanism of Phosphorescence Appropriate for the Long-Lasting Phosphors Eu^{2+} -Doped SrAl_2O_4 with Codopants Dy^{3+} and B^{3+} . *Chem Mater* 2005; 17: 3904-12.
- Ngaruiya JM, Nieuwoudt S, Ntwaeaborwa OM, Terblans JJ, Swart HC. Resolution of Eu^{2+} asymmetrical emission peak of $\text{SrAl}_2\text{O}_4:\text{Eu}^{2+}, \text{Dy}^{3+}$ phosphor by cathodoluminescence measurements. *Mater Letts* 2008; 62: 3192-4.
- Ryu H, Singh BK, Bartwal KS. Effect of Sr substitution on photoluminescent properties of $\text{BaAl}_2\text{O}_4:\text{Eu}^{2+}, \text{Dy}^{3+}$. *Physica B* 2008; 403: 126-30.
- Katsumata T, Sasajima K, Sasajima K, Komuro S, Morikawa T. Characteristics of Strontium Aluminate Crystals Used for Long-Duration Phosphors. *J Am Ceram Soc* 1998; 81: 413-16.
- Ju SH, Oh US, Choi JC, Park HC, Kim TW, Kim CD. Tunable color emission and solid solubility limit in $\text{Ba}_{1-x}\text{Ca}_x\text{Al}_2\text{O}_4:\text{Eu}^{2+,0.001}$ phosphors through the mixed states of CaAl_2O_4 and BaAl_2O_4 . *Mat Res Bull* 2000; 35: 1831-5.
- Zhao C, Chen D. Synthesis of $\text{CaAl}_2\text{O}_4:\text{Eu}, \text{Nd}$ long persistent phosphor by combustion processes and its optical properties. *Mater Lett* 2007; 61: 3673-5.
- Ryu H, Bartwal KS. Investigations on luminescence characteristics of Eu and Cr codoped BaAl_2O_4 . *Mater Chem Phys* 2008; 111: 186-9.
- Ryu H, Bartwal KS. Operation by Eu luminescence in $\text{CaAl}_2\text{O}_4:\text{Eu}^{2+}$ alloys by Zn substitution. *J Alloys Compd* 2008; 461: 395-8.
- Ryu H, Bartwal KS. Cr^{3+} doping optimization in $\text{CaAl}_2\text{O}_4:\text{Eu}^{2+}$ blue phosphor. *J Alloys Compd* 2008; 464: 317-21.
- Ryu H, Bartwal KS. Photoluminescence spectra of Nd^{3+} codoped $\text{CaAl}_2\text{O}_4:\text{Eu}^{2+}$ blue phosphor. *Res Lett Mater Sci* 2007; 2007: 1-4.